THE JOURNAL OF BIOLOGICAL CHEMISTRY
Vol. 278, No. 13, Issue of March 28, pp. 11676–11685, 2003

Printed in U.S.A.

MTA1 Interacts with MAT1, a Cyclin-dependent Kinase-activating Kinase Complex Ring Finger Factor, and Regulates Estrogen Receptor Transactivation Functions*

Received for publication, September 18, 2002, and in revised form, January 12, 2003
Published, JBC Papers in Press, January 13, 2003, DOI 10.1074/jbc.M209570200

Amjad H. Talukder‡§, Sandip K. Mishra‡§, Mahitosh Mandal‡, Seetharaman Balasenthil‡, Sonal Mehta‡, Aysegul A. Sahin¶, Christopher J. Barnes‡, and Rakesh Kumar‡‖

From the Departments of ‡Molecular and Cellular Oncology and ¶Pathology, The University of Texas M. D. Anderson Cancer Center, Houston, Texas 77030

The transcriptional activity of estrogen receptor-α is controlled by coregulators. MTA1 (metastasis-associated protein 1) represses estrogen receptor-α-driven transcription by recruiting histone deacetylases (HDACs) to the estrogen response element containing target gene chromatin in breast cancer cells. Using a yeast two-hybrid screen with the MTA1 C-terminal domain as bait, we identified MAT1 (ménage á trois 1) as an MTA1-binding protein. MAT1 is an assembly/targeting factor for cyclin-dependent kinase-activating kinase (CAK), which has been shown to functionally interact with general transcriptional factor TFIIH, a known inducer of ER transactivation. We show that estrogen signaling promotes nuclear translocation of MAT1 and that MTA1 interacts with MAT1 both *in vitro* and *in vivo*. MAT1 binds to the C-terminal 389–441 amino acids GATA domain and N-terminal 1–164 amino acids bromo-domain of MTA1, whereas MTA1 binds to the N-terminal ring finger domain of the MAT1. In addition, MAT1 interacts with the activation function 2 domain of ER and colocalizes with ER in activated cells. MTA1 deregulation in breast cancer cells led to its interactions with the CAK complex components, ER, and HDAC2. Accordingly, MTA1 inhibited CAK stimulation of ER transactivation that was partially relieved by HDAC inhibitor trichostatin A, suggesting that MTA1 might inhibit CAK-induced transactivation function of ER by recruiting HDAC. Furthermore, MTA1 overexpression inhibited the ability of CAK complex to phosphorylate ER. Together, these findings identified MAT1 as a target of MTA1 and provided new evidence to suggest that the transactivation functions of ER might be influenced by the regulatory interactions between CAK and MTA1 in breast cancer cells.

The eukaryotic genome is compacted with histone and other proteins to form chromatin, which consists of repeating units of nucleosome (1, 2). Formation of nucleosomes and higher order chromatin structures can render the DNA inaccessible to transcription factors and complexes. For transcription factors to access DNA, the repressive chromatin structure needs to be remodeled. Dynamic alterations in the chromatin structure can facilitate or suppress the access of the transcription factors to nucleosomal DNA, leading to transcriptional regulation. One way to achieve this is through alterations in chromatin remodeling factors or in the acetylation state of nucleosomal histones (3–5). Acetylation of core histones occurs at lysine residues on the N-terminal tails of the histones, thus neutralizing the positive charge of the histone tails and decreasing their affinity for DNA. Hyperacetylated chromatin is generally associated with transcription activation, whereas hypoacetylated chromatin is associated with transcription repression (3–6).

A number of recent studies have raised the possibility of a close connection between HDACs[1] and cancer. Because HDAC-mediated deacetylation of nucleosomal histones is known to be associated with transcriptional repression of some genes, it is being proposed that the deregulation of recruitment of HDAC-containing repressor complex to specific target promoters could serve as a potential mechanism by which these enzymes contribute to tumorigenesis. For example, MTA1 (metastasis-associated protein 1) represses estrogen receptor-α (ER)-driven transcription by recruiting HDAC to the ER response element (ERE)-containing target gene chromatin in breast cancer cells (7). The NuRD-70 polypeptide of nucleosome remodeling/HDAC complex is identical to that of the MTA1 (8–11). The MTA1 gene was initially identified by differential expression in rat mammary adenocarcinoma metastatic cells, and its expression has been shown to correlate well with the metastatic potential of several human cell lines and tumors (12).

To better understand the cellular functions of MTA1 in breast cancer cells, we performed a yeast two-hybrid screen to clone MTA1-interacting proteins. One of several isolates was identified as MAT1 (ménage á trois 1). MAT1 was originally discovered as an integral component of the cyclin-dependent kinase (CDK7)-activating kinase (CAK), a complex consisting of catalytic subunit CDK7, regulatory subunit cyclin H, and MAT1 (13). The MAT1 protein consists of three major motifs: the N-terminal RING finger region, the central coiled-coil region, and the C-terminal cyclin-like region (13–16). The functions of MAT1 are mediated by interactions of these motifs with distinct protein-protein interactions. For example, the RING finger domain is linked with general transcription factor TFIIH-mediated transcription (17), the coiled-coil domain in making contact with TFIIH via XPB and XPD helicase sub-

* This work was supported in part by National Institutes of Health Grant CA84456 and by Susan G. Komen Foundation Grant BCRT 2000835. The costs of publication of this article were defrayed in part by the payment of page charges. This article must therefore be hereby marked "*advertisement*" in accordance with 18 U.S.C. Section 1734 solely to indicate this fact.

§ These authors contributed equally to this study.

‖ To whom correspondence should be addressed: Dept. of Molecular and Cellular Oncology-108, The University of Texas M. D. Anderson Cancer Center, 1515 Holcombe Blvd., Houston, TX 77030.

[1] The abbreviations used are: HDAC, histone deacetylase; MTA1, metastasis-associated protein 1; ER, estrogen receptor-α; MAT1, ménage á trois 1; CAK, cyclin-dependent kinase-activating kinase; ERE, estrogen response element; E2, 17-β-estradiol; AF, activation function; CDK, cyclin-dependent kinase; ChIP, chromatin immunoprecipitation; GST, glutathione *S*-transferase; TSA, trichostatin A.

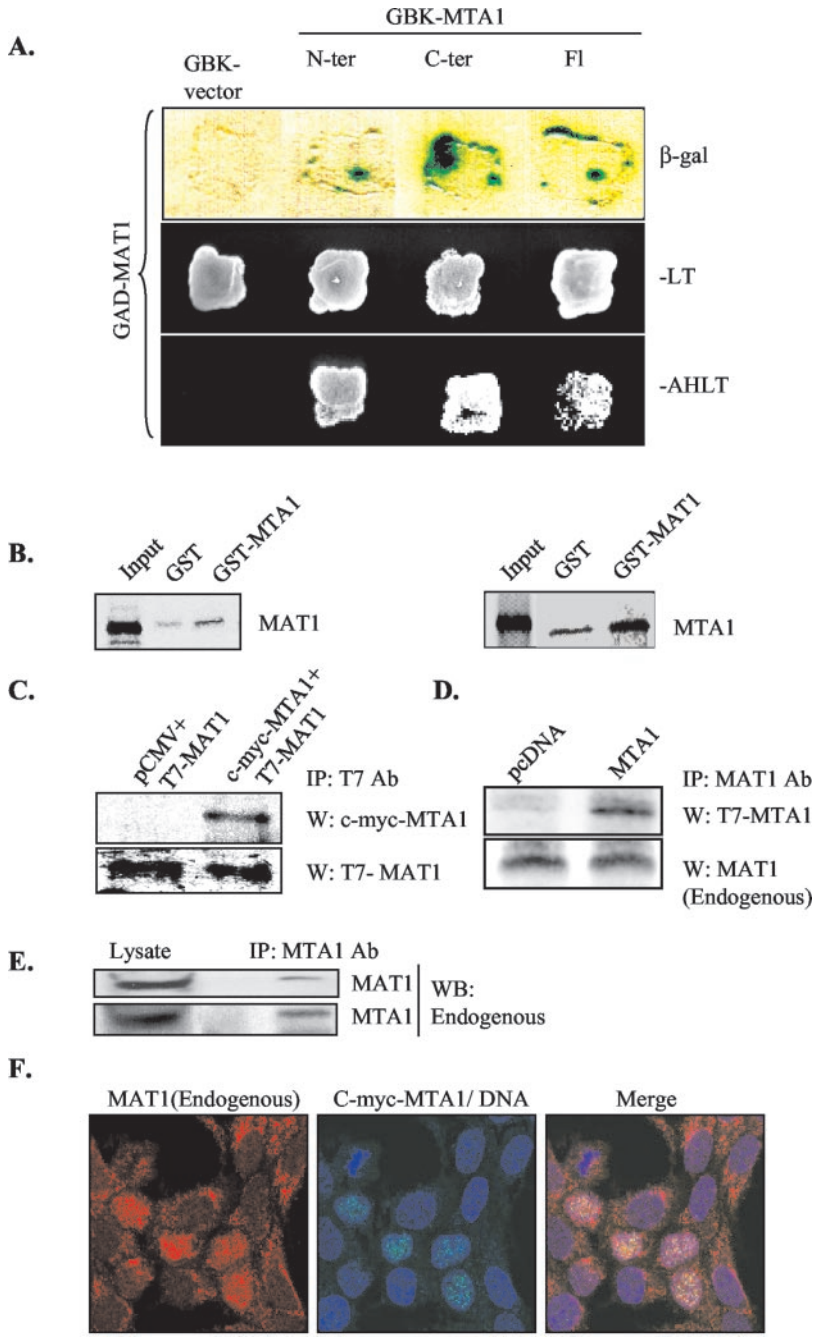

FIG. 1. **Identification of MAT1 as an MTA1-binding protein.** *A*, yeast cells were cotransfected with GAD-MAT1 and GBD control vector, or GBD-MTA1 (amino acids 1–715) or GBD-ctMTA1 (amino acids 255–715), or GBD-ntMAT1 (amino acids 1–173). Cotransformants were plated on selection plates lacking leucine and tryptophan (*−LT*) (*middle panel*) or lacking adenine, histidine, leucine, and tryptophan (*−AHLT*) (*bottom panel*). Growth was recorded after 72 h. For β-galactosidase assay, filter lift assays were performed. A *blue color* indicates the specific interaction of two proteins (*top panel*). *B*, MAT1 interaction in the GST pull-down assays. *In vitro* translated ^{35}S-labeled MAT1 protein was incubated with either MTA1-GST or GST (*left panel*), or *in vitro* translated ^{35}S-labeled MTA1 protein were incubated with either MAT1-GST or GST (*right panel*) and analyzed by SDS-PAGE and autoradiography. *C*, MCF-7 cells were cotransfected with Myc-MTA1 and T7-MAT1 or by T7-MAT1 and the pCMV vector. The cells were lysed after 36 h, immunoprecipitated with anti-T7 monoclonal antibody, resolved on 10% SDS-PAGE, and immunoblotted with anti-T7 and anti-Myc antibody. *D*, *in vitro* interaction between T7-MTA1 and MAT1. MCF-7/pCDNA and MCF-7/MTA1-T7 cells grown in 10% serum were lysed, and lysates containing equal amount of protein were immunoprecipitated with an anti-MAT1 monoclonal antibody and immunoblotted with antibodies against T7 and MAT1. *E*, endogenous MTA1 interacts with endogenous MAT1. Total protein from T47D cells was immunoprecipitated with anti-MTA1 antibody and immunoblotted with antibodies against either MAT1 or MTA1. *F*, MTA1 colocalizes with MAT1. MCF-7 cells were transiently transfected with c-Myc-MTA1, and fixed in methanol and immunofluorescently stained for c-Myc tag (*green*) and MAT1 (*red*) and counterstained for nuclear DNA (*blue*). Areas of colocalization of the *red* and *green* signals show *yellow* fluorescence (×40 magnification). *C-ter*, C-terminal; *N-ter*, N-terminal; *IP*, immunoprecipitation; *Fl*, full length; *W*, Western blot.

units (18), and the cyclin-like region in the formation of trimeric CDK7-cyclin H-MAT1 complex (19). MAT1 facilitates the formation of the ternary CAK complex by assembling and stabilizing the interactions between the CDK7 and cyclin H without involving the activating phosphorylation in the T-loop of human CDK7 (20). MAT1 has been also shown to determine the substrate specificity of CAK, because recruitment of MAT1 to the CDK7/cyclin H as a part of TFIIH preferentially targets the RNA polymerase II large subunit over CDK2 (21). In addition, MAT1 as a part of CDK7-cyclin H-MAT1 complex within the context of TFIIH enhances the phosphorylation of several *in vitro* substrates, including the POU domain of octamer transcription factor (22), tumor suppressor p53, and pRB proteins (23, 24), retinoic acid receptor-α (25, 26), and estrogen receptor-α (27). In addition, MAT1 also binds to XPB and XPD helicases subunits of TFIIH that recruit CAK complex to the core TFIIH (27). These observations suggest that MAT1 as a part of CAK in conjunction with multi-enzymatic protein complex TFIIH participates in several fundamental aspects of the transcription regulation. Because RING finger and coiled-coil motifs are generally involved in protein-protein interactions, MAT1 could potentially interact with other cellular regulatory proteins.

Here, we show that MTA1 directly binds to the MAT1 and represses CAK-mediated stimulation of ERE transcription and that MAT1 interacts with ER in a ligand-independent manner. In addition, MAT1 is frequently up-regulated in human breast tumors. These findings reveal a novel connection among MTA1, MAT1, and cancer and discovered the existence of regulatory interactions between MTA1 and CAK in breast cancer cells.

MATERIALS AND METHODS

Cell Cultures and Reagents—MCF-7, MDA-MB-231, T47-D, MDA-MB-453, BT-474, and ZR-75 human breast cancer cells (7, 28) were maintained in Dulbecco's modified Eagle's medium supplemented with 10% fetal calf serum. The following antibodies were used: anti-MAT1, anti-MTA1, anti-cyclin H, anti-CDK7, and anti-HDAC1 (Santa Cruz

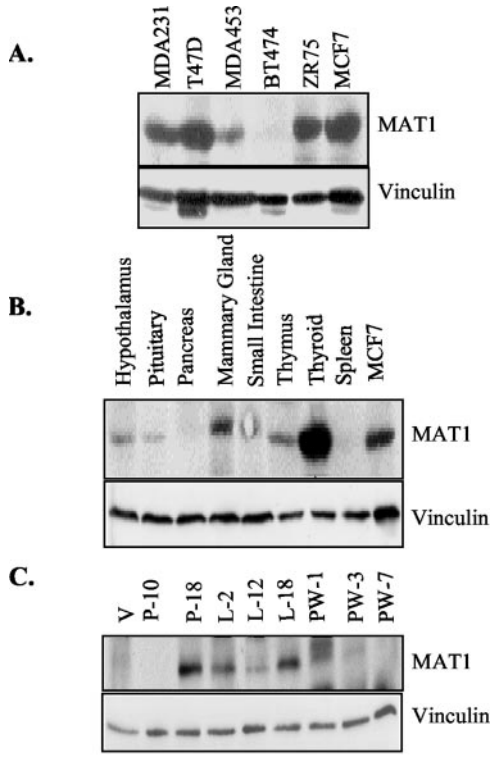

FIG. 2. **MAT1 expression in different cells and normal mouse tissues.** *A*, MTA1 expression in human breast cancer cells. *B*, MAT1 expression in normal mouse tissues was detected by immunoblotting with the indicated antibodies. *C*, MTA1 expression during the different stages of murine mammary gland development. *V*, virgin; *P*, pregnancy; *L*, lactation; *PW*, post-weaning. *Numbers* represent days.

Biotechnology, Santa Cruz, CA), anti-T7 (Novagen, Milwaukee, WI), anti-HER-2 (NeoMarkers, Fremont, CA), anti-vinculin (Sigma), anti-ER (Upstate Biotechnology, Lake Placid, NY), and anti-mouse horseradish peroxidase conjugate (Amersham Biosciences). Alexa 546-labeled goat anti-rabbit and Alexa 488-labeled goat anti-mouse secondary antibodies and the DNA-intercalating fluorescent dye ToPro3 were purchased from Molecular Probes (Eugene, OR).

Plasmid Construction and Two-hybrid Library Screening—The full-length MTA1 (1–715 amino acids) (7) was digested with *Bam*HI and *Xba*I (blunt end) and ligated to the pGBKT7 vector that expresses protein fused to amino acids 1–147 of the GAL4-DNA binding domain at *Bam*HI and *Pst*I (blunt end) (Clontech). MTA1 baits were constructed by deleting 1–254 amino acids from the N terminus of MTA1 by cutting and self-ligating with *Nco*I. The remaining 255–715 amino acids of the C terminus of MTA1 was used as bait. This bait was used to screen a human mammary gland cDNA library fused to the Gal4 activation domain (Clontech) according to the manufacturer's instructions. A total of 2×10^6 clones were screened. The positive clones were isolated and sequenced at the University of Texas M. D. Anderson Cancer Center Core sequencing facility. The positive clones were also verified by one-on-one transformations and selection on agar plates lacking adenine, histidine, tryptophan, and leucine and also by β-galactosidase assay (28).

Deletion Constructs of MTA1 and MAT1—Nine MTA1 deletion constructs were generated to map the binding site(s) of MTA1 with MAT1 by PCR-based procedure. Starting from the N-terminal region, the constructs were named N1-MTA1 to N9-MTA1. All of the forward (F) primers including the ATG start codon primer contain an *Eco*RI site and all of the reverse (R) primers including the stop codon (TAG) primer contain a *Sal*I site. The ATG start codon primer is 5′-GCCGCCGGAATTCACATGGCCGCCAACA-3′and the stop codon (TAG) primer was 5′-AGGTGGGGGTCGACCCTAGTCCTCCCG-3′. The construction of N1-MTA1 through N7-MTA1 used the ATG start codon primer plus N1R, 5′-ACTCGAATGTCGACTTTATCTGCCA-3′; N2R, 5′-AGCTGCTG-CAGTCGACGGCCCGTGCGA-3′; N3R, 5′-AGGCCCGGCCGTCGA-CAGGGCTCTGGCCCGG-3′; N4R, 5′-ACTGCGGTGTCGACCTGGC-CTCTCTCCA-3′; N5R, 5′-ACCGAAGCACGTCGACCAGCGGCTT-3′;

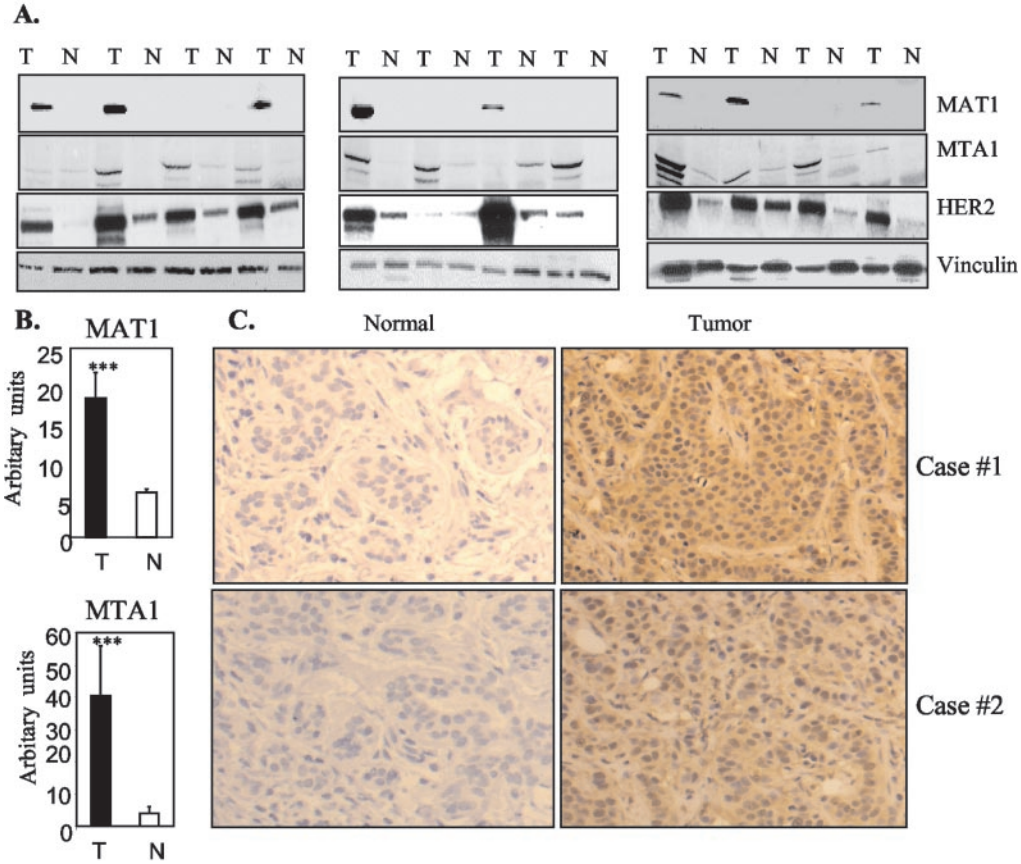

FIG. 3. **MAT1 expression in human breast tumors.** *A*, paired breast tumors (*T*) and adjacent normal (*N*) tissue were analyzed by immunoblotting with the indicated antibodies. *B*, densitometric quantitation of MTA1 and MAT1 signals. *C*, representative immunohistochemical staining for MAT1 in tissues from normal and tumor sections. The tumor section shows both nuclear and cytoplasmic staining.

and N6R, 5′-TCAGGCGCACGTCGACGGGGTAGGACT-3′, respectively. The N7-MTA1 was constructed by using N7F, 5′-ACCTTCGGAATTCCCCTGGACTGCA-3′, and N3R primers. For the construction of N8-MTA1 (422–715 amino acids) and N9-MTA1 (542–715 amino acids), we used stop codon primer and N8F, 5′-TGATGGAGGAATTCCAGGACCAAAC-3′, and N9F, 5′-GAAGCCGTGCGAATTCATCTTGAGA-3′, respectively. All of the PCR products were run into 0.8% agarose gel, purified by Geneclean or Mermaid (Bio 101, Inc., Vista, CA), cut with *EcoR1* plus *Sal*I, and ligated to pGEX-5X vector at *EcoR1* and *Xho*I site. After confirming the sequences, these constructs were cut at *Eco*RI and *Not*I site and ligated with pcDNA3.1A vector at *Eco*R1 and *Not*I site for the T7 tag protein (29). The sequence of N10-MTA1 deletion construct (amino acids 212–715) has been described previously (28).

A similar PCR-based procedure was used to generate eight deletion constructs of MAT1. Four of five deletion constructs were made for MAT1 using either start codon primer 5′-GGGAATTCCCATGGACGATCAGGGT-3′ or stop codon primer 5′-CTTATGTCGACTTAA CTGGGCTGCCA-3′. The following constructs were made by PCR with start codon primer plus 189R (1–189 amino acids), 5′-GCAGAGCAACAGCGGCCGCAGAAC TCTCCAGCTCAT-3′; 114R (1–114 amino acids), 5′-TCTTTTTGGTGGCGGCCGCATCCACATTGTTG-3′; 66R (1–66 amino acids), 5′-CAACCTCCTTGGCGGCCGCGGGATCTTCAAAGA-3′; and using stop codon primer plus 189F (189–309 amino acids), 5′-GATGAGCTGGGAATTCCTGATCTCCCTGTTGCT-3′. The amino acids 114–189 construct was made using the primers 114F, 5′-ACTTGACCAACAGAATTCATTTGGACAACACCA-3′, and 189R. After Geneclean, the PCR products were digested with either *Eco*R1 and *Sal*I or *Eco*R1 and *Not*I and ligated to a pcDNA 3.1A vector at either *Eco*RI and *Xho*I or *Eco*RI and *Not*I.

Transfection, Cell Extracts, and Immunoprecipitation—Transfection was performed with a FuGENE 6 kit (Roche Molecular Biochemicals) according to the manufacturer's instructions. The cells were lysed with RIPA buffer supplemented with 100 mM NaF, 2 mM $NaVO_5$, 1× protease mixture (Roche Molecular Biochemicals) on ice for 15 min. Cell lysates containing equal protein were immunoprecipitated with the desired antibody and analyzed by SDS-PAGE (28, 29).

CAK Phosphorylation of ER—The effect of MTA1 on CAK phosphorylation of ER was determined according to Chen *et al.* (27). Briefly, MCF-7 cells stably expressing either pcDNA or T7-MTA1 were transfected with CDK7 and MAT1 and labeled with [^{32}P]orthophosphoric acid. The cell lysates were immunoprecipitated with an anti-ER antibody, and the status of phosphorylated ER was analyzed by autoradiography.

Chromatin Immunoprecipitation (ChIP) Assay—Approximately 10^6 cells were treated with cross-linked histones to DNA. The ChIP assay was performed as described (7). After immunoprecipitation with corresponding antibodies, the eluted DNA was amplified by PCR using the primers GAATTAGCTTAGGCCTAGACGGAATG (forward) and AGGATTTGCTGATAGACAGAGACGAC (reverse) for pS2 promoter around the ERE site.

Tissue Samples and Western Blotting—Mouse tissue samples were collected and snap frozen in liquid nitrogen as described previously (7, 30). Human breast tissue samples were obtained from the University of Texas M. D. Anderson Breast Tumor Core Pathology Laboratory maintained by Aysegul A. Sahin (31, 32). Thawed tissue samples were homogenized in Triton X-100 lysis buffer (20 mM HEPES, 150 mM NaCl, 1% Triton X-100, 0.1% deoxycholate (v/w), 2 mM EDTA, 2 mM $NaVO_5$, and protease inhibitor mixture), and equal amounts of protein were analyzed by Western blotting. The protein vinculin was used routinely as a loading control.

In Vitro Transcription, Translation, and GST Pull-down Assays—*In vitro* transcription and translation of the test proteins were performed by using the TNT transcription-translation system (Promega). One microgram of desired DNA in pCDNA 3.1 vector (Invitrogen) was translated in the presence of [^{35}S]methionine in a reaction volume of 50 μl by using the T7-TNT reaction mixture. The reaction mixture was diluted to 1 ml with Nonidet P-40 lysis buffer, and an aliquot (250 μl) was used for each GST pull-down assay. Two μl of the translated reaction mixture was verified by SDS-PAGE and autoradiography. The GST pull-down assays were performed by incubating equal amounts of GST or GST fusion protein immobilized to glutathione-Sepharose beads (Amersham Biosciences) with *in vitro* translated ^{35}S-labeled test protein. The mixtures were incubated for 2 h at 4 °C and washed six times with Nonidet P-40 lysis buffer. The bound proteins were eluted with 2× SDS buffer, separated by SDS-PAGE, and visualized by fluorography (32).

Immunofluorescence and Confocal Imaging—The cells were plated on glass coverslips in 6-well culture plates. When the cells were ~50% confluent, they were serum-starved for 36 h. Alternatively, 30% confluent cells were maintained in phenol red-free medium supplemented with 5% charcoal-striped fetal calf serum for 72 h and treated with β-estradiol (10^{-9} M) for 30 min with or without pretreatment with the anti-estrogen ICI 182780 (10^{-8} M) for 1 h. The cells were rinsed in phosphate-buffered saline, fixed in cold 100% methanol for 10 min, and processed for immunofluorescent localization of MAT1 and Myc-tagged MTA1 or ER. The DNA was visualized by counterstaining with ToPro3. Fluorescent labeling was visualized using a Zeiss LSM 510 microscope and a 40× objective (32).

Immunohistochemistry—For immunohistochemical detection of MAT1, the sections were deparaffinized with xylene and rehydrated using graded ethanol (30). The sections were incubated in 0.3% H_2O_2 and methanol for 30 min to inactivate endogenous peroxidase. The sections were then boiled for 10 min in 0.01 M citrate buffer and cooled for 30 min at room temperature to expose antigenic epitopes. The sections were sequentially biotin- and protein-blocked and incubated

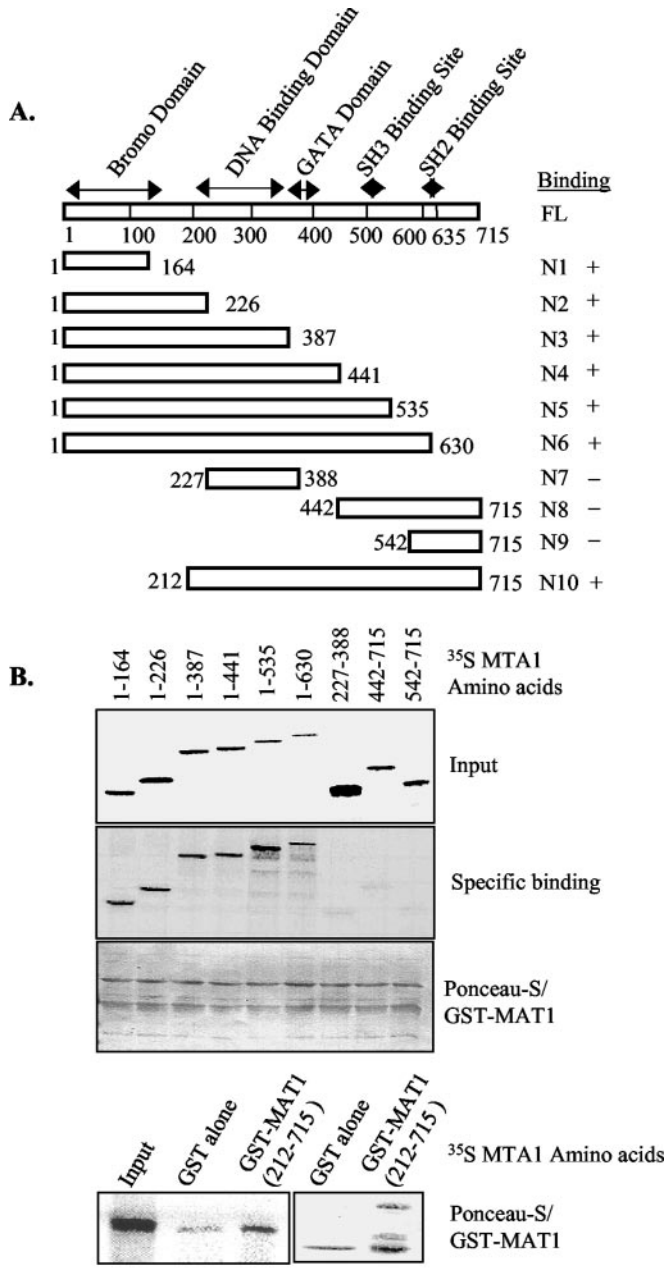

FIG. 4. **Mapping of MTA1 interaction domains of MAT1.** *A*, schematic representations of MAT1 constructs. *N1*, amino acids 1–164; *N2*, amino acids 1–226; *N3*, amino acids 1–387; *N4*, amino acids 1–441; *N5*, amino acids 1–535; *N6*, amino acids 1–630; *N7*, amino acids 227–388; *N8*, amino acids 442–703; *N9*, amino acids 542–703; and *N10*, amino acids 212–715. *B*, GST pull-down assays using ^{35}S-labeled *in vitro* translated MAT1 polypeptides and GST-MTA1 proteins.

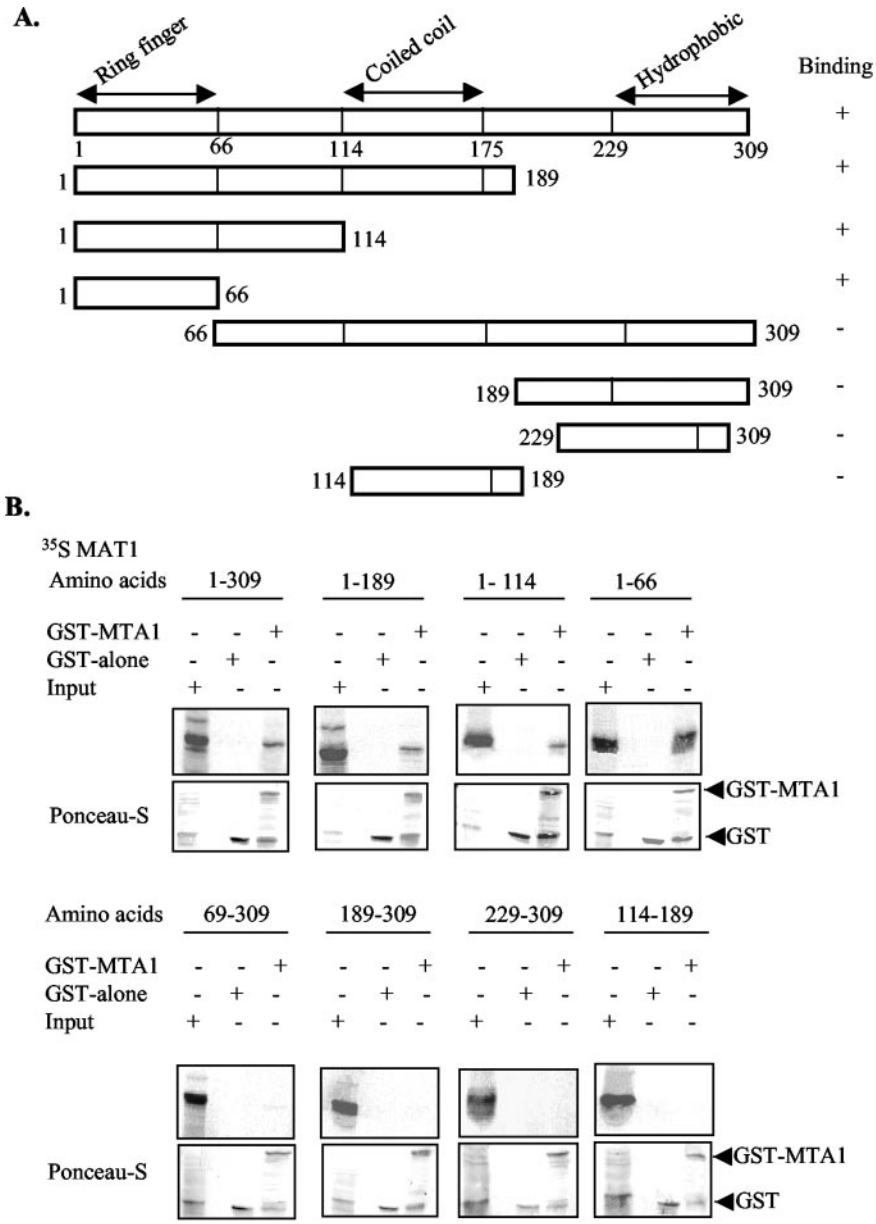

FIG. 5. **Mapping of MAT1 interaction domains of MTA1.** *A*, schematic representations of MAT1 constructs representing amino acids 1–189, 1–114, 1–66, 66–309, 189–309, 229–309, and 114–189. *B*, GST pull-down assays using ^{35}S-labeled *in vitro* translated MAT1 polypeptides and GST-MTA1 protein.

with primary antibody overnight at room temperature followed by biotinylated secondary antibody, streptavidin-biotin complex, amplification reagent, and streptavidin-peroxidase complex (DAKO Corporation, Carpinteria, CA), and then developed with DAB-H_2O_2 and counterstained with Mayer's hematoxylin. Anti-MAT1 antibody (Santa Cruz Biotechnology, Santa Cruz, CA) was used at a dilution of 1:100.

Statistical Analysis—Statistical analysis was done using Student's *t* test. The values are considered statistically significant if $p < 0.05$.

RESULTS

Identification of MAT1 as a MTA1-interacting Protein—To better understand the functions of MTA1 in breast tumor cells, a yeast two-hybrid screening of the mammary gland cDNA expression library was performed using the MTA1 C-terminal amino acids 255–715 as bait. This bait contains several binding motifs (DNA-binding domain, GATA domain, and SH2 and SH3 binding domains). As a negative control, we used a recently identified MTA1s variant that lacks protein-binding motifs as bait (28). Yeast cells expressing the Gal4 fusion protein were transformed with the above bait. Screening of 2×10^6 transformants resulted in the isolation of several positive clones. By sequencing of the positive clones, we identified several clones that encoded cDNA of MAT1 (GenBank™ accession number X92669), an integral component of the CAK complex (33). The specificity of the MTA1-MAT1 interactions was verified by one-on-one transformation (Fig. 1*A*). Interaction was further confirmed by the growth of the transformed colonies in medium lacking adenosine, histidine, tryptophan, and leucine and development of blue coloration in β-galactosidase assay, whereas the cotransfection with the control GBK vector did not do so (Fig. 1*A*). Subsequent studies were undertaken to understand the significance of MTA1 interactions with MAT1 in breast cancer cells.

MAT1 Interacts with MTA1 in Vitro—To confirm the interaction between MAT1 and MTA1, we next examined the ability of *in vitro* translated MAT1 protein to bind with GST-MTA1 *in vitro*. MAT1 interacted efficiently with GST-MTA1 but not with GST alone in GST pull-down assays (Fig. 1*B*, *left panel*). Conversely, *in vitro* translated MTA1 protein also specifically interacted with GST-MAT1 (Fig. 1*B*, *right panel*).

MAT1 Interacts with MTA1 in Vivo—To confirm the MAT1 interaction with MTA1 *in vivo*, MCF-7 cells were cotransfected with the equal amounts of c-Myc-tagged MTA1 and T7-tagged MAT1. Immunoprecipitation of cell lysates with an anti-T7

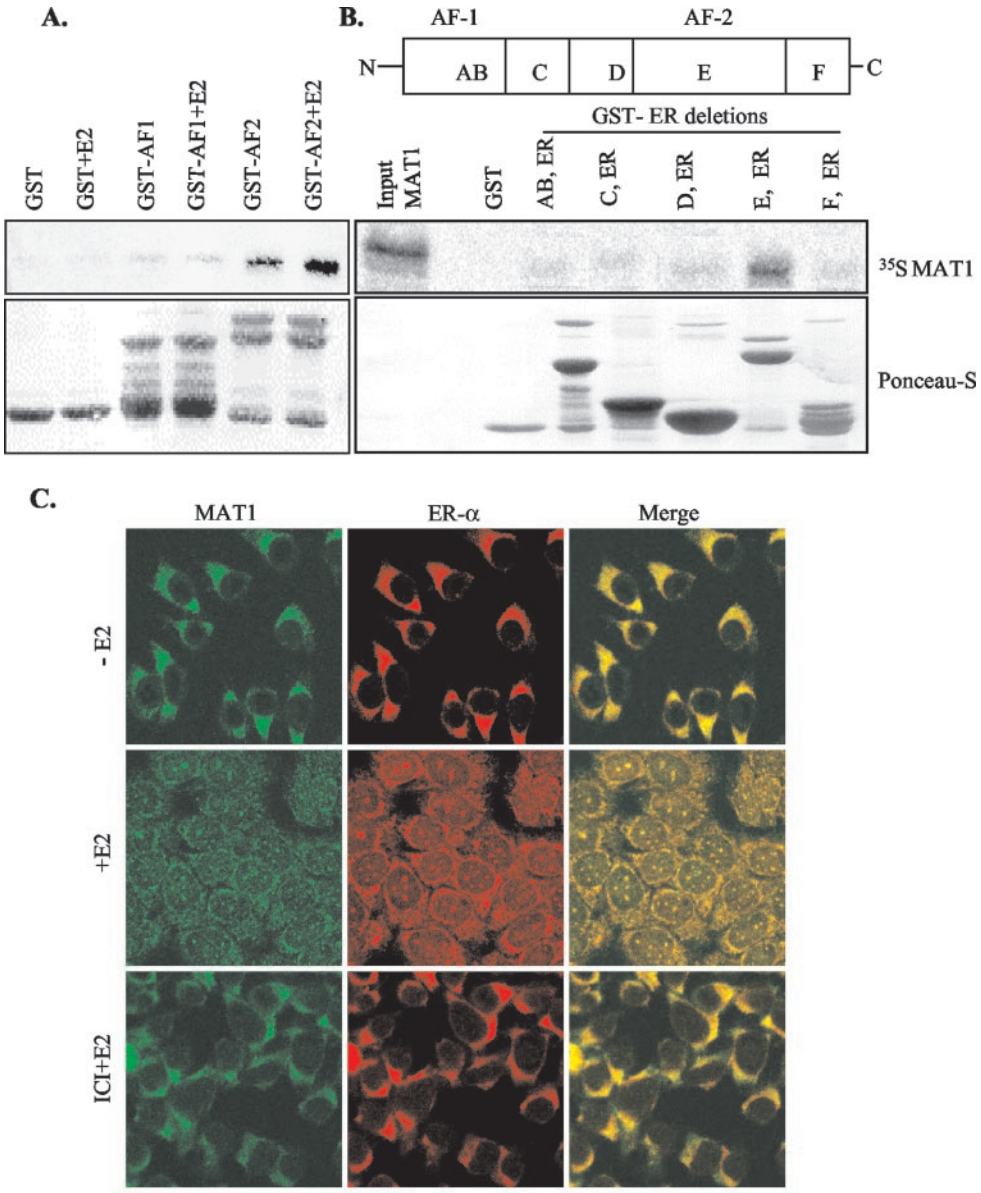

FIG. 6. **MAT1 interaction with ER.** *A*, GST pull-down assay involving *in vitro* translated ^{35}S-MAT1 was incubated with GST-AF1 or GST-AF2 or GST in the presence and absence of E2. *B*, GST fusion proteins from five functional domains of ER were incubated with *in vitro* translated ^{35}S-MAT1 and analyzed by SDS-PAGE and autoradiography. *C*, MAT1 and ER colocalize following estradiol treatment. MCF-7 cells were grown in phenol red-free medium supplemented with 3% charcoal-stripped serum for 72 hours and then treated with E2 for 30 min. The cells were fixed in methanol and immunofluorescently stained for MAT1 (*green*) and estrogen receptor (*red*). Areas of colocalization of the *red* and *green* signals show *yellow* fluorescence. Control cells, MAT1, and ER were diffusely localized in the cytoplasm. E2-treated cells, MAT1, and ER show strong colocalization at the nuclear periphery and in specific intranuclear regions (×40 magnification).

antibody was followed by immunoblotting with anti-c-Myc antibody. As illustrated in Fig. 1*C*, cotransfection with T7-MTA1 but not pCDNA coimmunoprecipitated c-Myc-MTA1. To further demonstrate the existence of the noticed interaction between MAT1 and MTA1 *in vivo*, we used MCF-7 breast cancer cells stably expressing T7-tagged MTA1 or pCDNA (7). Immunoprecipitation of the endogenous MAT1 with an anti-MAT1 monoclonal antibody was followed by immunoblotting with the anti-T7 monoclonal antibody. The results showed specific interaction between the endogenous MAT1 and T7-MTA1 in MCF7/MTA1 cells but not in MCF7/pCDNA cells (Fig. 1*D*). Next, we used T47D breast cancer cells that express both MAT1 as well as MTA1 to demonstrate the interaction between the endogenous MAT1 and MTA1. Immunoprecipitation of lysate from exponentially growing cells with anti-MTA1 antibody was followed by Western blotting with anti-MAT1 antibody. The results show that endogenous MTA1 and endogenous MAT1 do interact with each other (Fig. 1*E*).

To explore the spatial relationship between MTA1 and MAT1 and further validate their interactions *in vivo*, we utilized immunofluorescence and confocal scanning microscopy. MCF-7 cells were transiently transfected with Myc-tagged MTA1 and stained using antibodies against c-Myc antibody to detect c-Myc-MTA1 (*green*) or anti-MAT1 antibody to detect the endogenous MAT1 (*red*), and DNA was counterstained with the DNA dye Tropo3 (*blue*). Areas of colocalization of the red and green signals show yellow fluorescence (Fig. 1*F*). In nontransfected cells, MAT1 protein was spread diffusely in the cytoplasm and absent from the nucleus (Fig. 1*F*). This result is in agreement with previous reports on the subcellular distribution of MAT1 (33). Transfected MTA1 was concentrated in the nucleus, as expected (7). Importantly, MAT1 was also concentrated in the nucleus selectively in Myc-MTA1 transfected cells, where it colocalized with Myc-MTA1 (Fig. 1*F*, *right pan-*

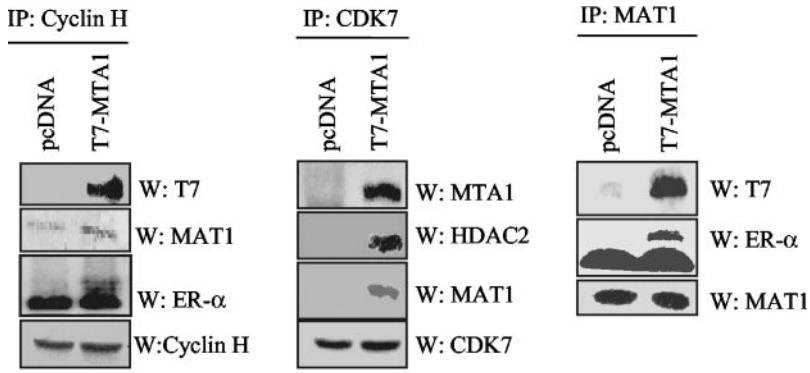

FIG. 7. **MTA1 interacts with CAK components and ER.** Lysates from MCF-7/pCDNA and MCF-7/T7-MTA1 cells (7) were immunoprecipitated with antibodies against cyclin H, CDK-7, or MAT1 and immunoblotted with the indicated antibodies. *IP*, immunoprecipitation; *W*, Western blot.

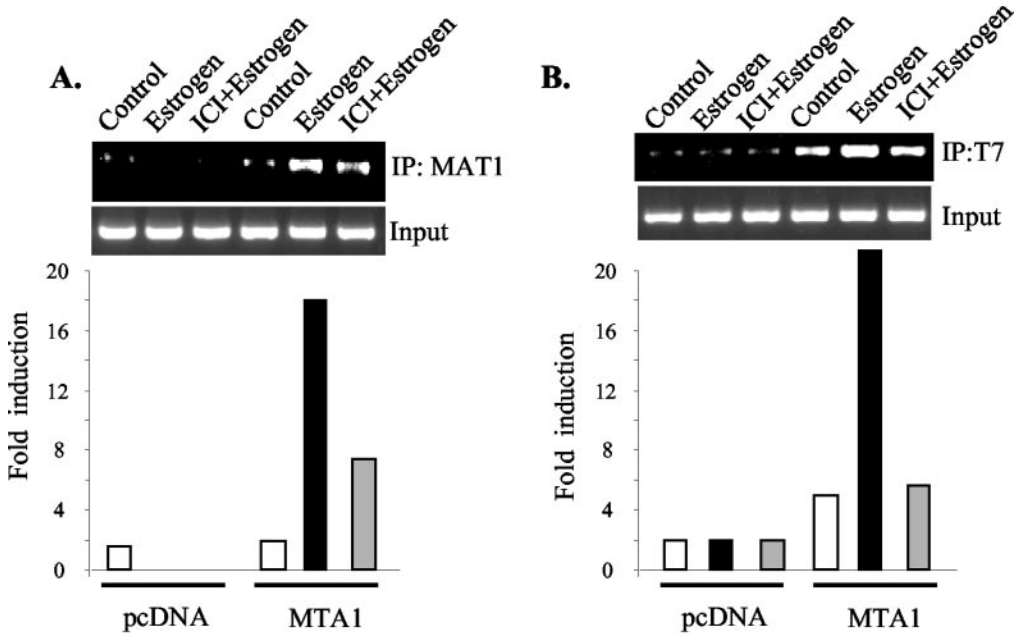

FIG. 8. **MAT1 interacts with ER target gene chromatin.** *A*, MCF-7/T7-MTA1 cells (7) treated with estrogen (10^{-9} M) for 3–6 h. Then cells were cross-linked and processed for ChIP assay by using anti-MAT antibody, and PCR was performed. *B*, MCF-7/pCDNA and MCF-7/T7-MTA1 cells were treated either with estrogen for 3–6 h or with ICI (10^{-7} M) for 1 h and then with estrogen for 3–6 h. Subsequently, the cells were processed for ChIP assay by using anti-MAT antibody or anti-T7 antibody, and PCR was performed. *IP*, immunoprecipitation.

el). Together, these observations suggested that MAT1 could interact with Myc-MTA1 under physiological conditions, suggesting the possible influence of MTA1 on the functions of MAT1 in breast cancer cells.

MAT1 Expression Pattern—To explore the significance of MAT1 in breast tissues, we examined MAT1 protein expression levels in normal mouse tissues and human breast cancer cell lines. MAT1 protein was easily detectable in both ER-positive (MCF7, ZR75 and T47D) and ER-negative (MDA-MB231, MDA-MB453 and BT474) cell lines (Fig. 2*A*). As shown in Fig. 2*B*, various levels of MAT1 protein were present in many mouse tissues, with the highest level in the thyroid and mammary glands of pregnant mice (Fig. 2*C*). To explore the significance of MAT1 in human breast tumors, we investigated whether MAT1 protein expression was altered in paired normal human breast epithelium and breast carcinoma biopsy samples. As shown in Fig. 3*A*, MAT1 expression was elevated in 8 tumors of 12 as compared with the adjacent normal tissue, which showed either or no expression of MAT1. In 6 of the MAT1-overexpressing tumors, there was also up-regulation of MTA1. The blots were reprobed for vinculin as a loading control. Densitometric scanning of MAT1 and MTA1 protein bands suggested the existence of statistically significant up-regulation of both proteins in breast tumors as compared with adjacent normal appearing tissues (Fig. 3*B*). To validate these results, we immunostained paraffin-embedded paired tissue specimens with an anti-MAT1 monoclonal antibody. Two representative examples in Fig. 3*C* demonstrate an intense MAT1 nuclear staining in tumor tissue, and normal tissue showed no positive staining.

Mapping of MAT1- and MTA1-interacting Domains—Next, we defined the minimal region of MTA1 required for its interaction with MAT1. MTA1 has several important domains involved in protein-protein interactions, DNA binding, and signaling (Fig. 4*A*). Several C-terminal MTA1 deletion constructs were generated and expressed as ^{35}S-labeled proteins and then subjected to GST pull-down assays with the GST-MAT1 fusion proteins. The results suggest that amino acids 1–164 of MTA1, which contain the bromo-domain, and 389–441 amino acids representing the GATA domain constitute the binding regions for MAT1 (Fig. 4*B*). To define the binding region or regions of MAT1 that are important for MTA1 interaction, we generated MAT1 encompassing different regions such as N-terminal RING finger region, the central coiled-coil region, and the C-terminal cyclin-like box (Fig. 5*A*). The results of the GST pull-down assays indicated that MAT1 uses amino acids 1–66 (representing the ring finger domain) to interact with MTA1 efficiently (Fig. 5*B*). These findings demonstrated that MAT1

binds to the C-terminal 389–441 amino acids GATA domain and N-terminal 1–164 amino acids bromo-domain of MTA1, whereas MTA1 binds to the N-terminal ring finger domain of the MAT1.

MAT1 Interacts with ER—Because repressed MTA1 has been shown to shown to repress the transactivation functions of ER (7), we hypothesized that MAT1 might physically interact with ER and influence its function. To explore this possibility, we examined the binding ability of *in vitro* translated MAT1 protein and with the GST-AF1 and AF2 domains of ER in GST pull-down assays. As shown in Fig. 6*A*, MAT1 protein effectively interacted with the GST-AF2 (ligand-binding domain of ER) but not with GST alone or GST-AF1, and this binding was further increased significantly in the presence of estrogen. To confirm these results, we performed GST pull-down assays using various deletion mutants of ER representing domains of ER and showed that MAT1 interacts with the ligand-binding region of ER (Fig. 6*B*).

To determine whether MAT1 and ER would colocalize *in vivo*, we examined the immunolocalization of these proteins by confocal microscopy. MCF-7 cells were grown in estrogen-free medium for 72 h and then were treated with E2 (10^{-9} M) for 30 min. In hormone-depleted cells, both MAT1 (endogenous) and ER were diffusely localized in the cytoplasm and absent from the nucleus (Fig. 6*C*, *top panels*). However, after E2 treatment, there was a rapid movement of both proteins to the nuclear periphery, concentration in specific nuclear regions, and also diffuse localization in the nucleus (Fig. 6*C*, *middle panels*). Pretreatment of cells with the pure anti-estrogen compound ICI 182780 completely blocked this dramatic estrogen effect on MAT1 and ER intracellular localization (Fig. 6*C*, *bottom panels*), confirming the ER-mediated nature of the noticed nuclear colocalization of MAT1 and ER.

MTA1 Interacts with CAK Complex Components—The CAK complex is composed of CDK7, cyclin H, and MAT1. To demonstrate the endogenous interaction of MTA1 with the components of CAK complex, cell lysates from exponentially growing MCF-7/T7-MTA1 and MCF-7/pcDNA cells (7) were immunoprecipitated with antibodies against cyclin H, CDK7, and MAT1. As shown in Fig. 7, MTA1 could be detected in complexes consisting of cyclin H, CDK7, and MAT1 only in MCF-7/T7-MTA1 and not in vector-transfected MCF-7 cells. Interestingly, both ER and HDAC2 were also present in the CAK1-MTA1 complex, suggesting a potential role for MTA1 in modifying (*i.e.* repressing) the effect of CAK on the transactivation functions of ER.

MAT1 Associates with the ERE-responsive Promoters in Vivo—To directly demonstrate the potential importance of MTA1-MAT1 interaction in ERE transcription, we used the ChIP assay to analyze whether T7-MTA1 or MAT1 associates with the endogenous ERE-containing promoters. MCF-7/pcDNA and MCF-7/T7-MTA1 cells were treated with E2 in the presence or absence of ICI 182780 for 30 min and processed to formaldehyde cross-link and to sonicated chromatin for immunoprecipitation with specific antibodies against T7 or MAT1. T7-MTA1 or MAT1-bound genomic DNA fragments were analyzed by quantitative PCR using primers spanning the ERE elements present in the promoter of the pS2 sequence. The results indicated that E2 treatment triggered a significant increase in the amount of pS2 target gene promoter chromatin associated with T7-MTA1 or MAT1 (Fig. 8). Because both MAT1 and MTA1 interacted effectively with the ER target gene chromatin, these findings raised the possibility that MTA1 might influences the status of ER transactivation by MAT1 as a part of CAK complex. In brief, these findings from Figs. 6 and 8 strongly support the notion that MTA1 might influence the

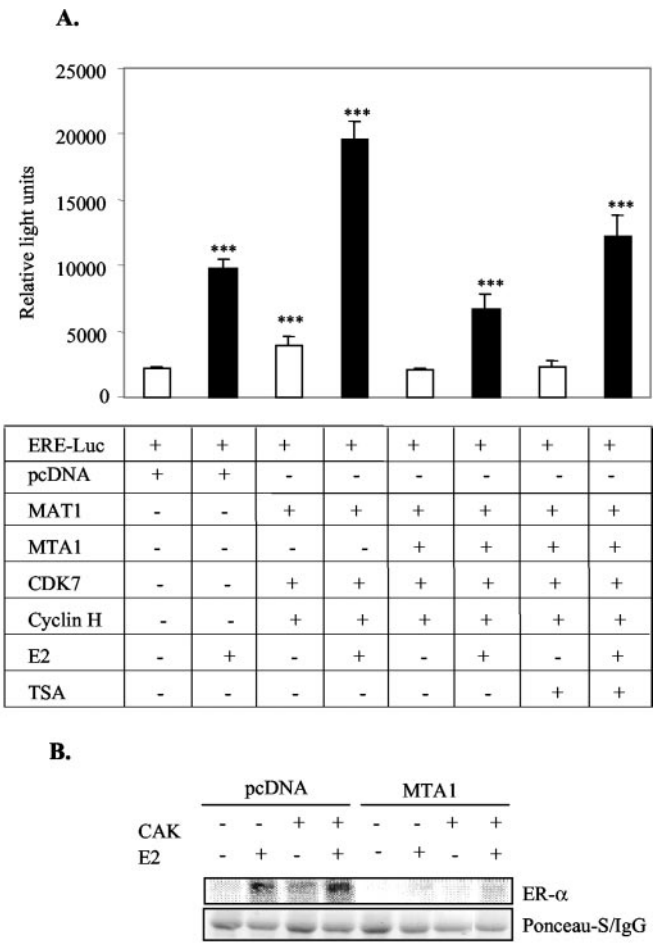

FIG. 9. **MTA1 inhibits CAK-mediated ER transactivation.** *A*, MCF7 cells were cotransfected with 0.25 μg of ERE-luciferase reporter, 0.5 μg of MAT1, 0.5 μg of MTA1, 0.5 μg of CDK7, and 0.5 μg of cyclin H with or without estrogen or TSA stimulation. After 36 h, the cells were lysed, and luciferase activity was measured (n = 3). The activity was normalized with β-galactosidase activity. *B*, stable clones overexpressing pcDNA or MTA1 were transfected with vector alone or CDK7, cyclin H and MAT1. The cells were maintained in phosphate-free medium before adding [^{32}P]orthophosphoric acid to the medium. After 36 h of transfection, the cells were either treated with ethanol or estradiol (10^{-9} M, 2 h). Subsequently cells were lysed and immunoprecipitated with anti-estrogen receptor antibody, resolved on a 8% SDS-PAGE, and taken for autoradiography.

regulation of ER transactivation function by CAK1-associated mechanisms.

MTA1 Inhibits CAK Stimulation of ER Transactivation—To assess the potential significance of noticed MTA1-MAT1 interactions, we next examined the effect of MTA1 on the ability of CAK to ER transactivation function in MCF-7 cells. Previous reports have shown that coexpression of all three components but not individual subunits of CAK1 stimulate transcriptional activity of ER in HeLa cells (27). Consistent with these observations, we observed a significant stimulation of ERE-dependent transcription by CAK1 in MCF-7 cells (Fig. 9*A*). Interestingly, MTA1 expression blocked the ability of CAK1 to ER-mediated ERE transactivation. Because MTA1 interacts with HDAC2 (7) and because HDAC2 could be detected in MTA1/CAK1 (Fig. 7) in breast cancer cells, we reasoned that HDAC inhibition by TSA might relieve the inhibitory effect of MTA1 on CAK1. Indeed, TSA treatment of cells was accompanied by a considerable derepression by MTA1. These findings suggested that MTA1 might inhibit CAK-induced transactivation function of ER by recruiting HDAC.

To further understand the role of MTA1 in the functions of CAK, we next examined the effect of MTA1 deregulation on the CAK activity as determined by its ability to phosphorylate ER *in vivo*. MCF-7 expressing pcDNA or MTA1 cotransfected with MAT1 and CDK7 were labeled with [^{32}P]orthophosphoric acid. The cell lysates were immunoprecipitated with an anti-ER antibody and analyzed by autoradiography. As expected from the previous work by Chen *et al.* (27), CAK expression in MCF7/pcDNA cells was accompanied by increased phosphorylation of ER (compare *lane 3* with *lane 1*), which could be further increased by estrogen treatment (Fig. 9*B*, compare *lane 4* with *lanes 3* and *2*). Interesting, the CAK failed to phosphorylate ER in MCF7/MTA1 cells in both the absence and the presence of estrogen stimulation (Fig. 9*B*). These results suggested that MTA1 deregulation could also impair the ability of CAK to phosphorylate ER.

DISCUSSION

In the present study, we have identified MAT1, an essential component of CAK complex with functions in cell cycle control and transcription, as a MTA1-interacting protein using the yeast two-hybrid screening. We show that MTA1 interacts with MAT1 both *in vitro* and *in vivo* and that MTA1 could be detected in a complex consisting of CAK components ER and HDAC in breast cancer cells. In an attempt to understand the significance of these biochemical interactions, we followed an earlier finding showing that the CAK complex enhances the ER transactivation function (27) and demonstrated that estrogen stimulation of breast cancer cells promotes rapid nuclear translocation of MAT1 and its association with the endogenous ER. Using recombinant proteins, we further demonstrated that MAT1 directly interacts with the AF2 domain of ER under basal as well as E2-inducible conditions. In the context of MTA1, we show that both MTA1 and MAT1 associate with the ER target gene pS2 promoter chromatin and that MTA1 inhibits its CAK-induced stimulation of transactivation function of ER. The functional significance of these findings is derived from the observations that MAT1 acts as the assembly and targeting factor of CAK, which regulates transcription including transactivation property of ER (27). Because MTA1 expression is deregulated in human breast tumors (28), it is possible that MTA1 up-regulation might suppress CAK regulation of the transactivation activity of ER and, subsequently, leads to loss of ER responses, which is generally associated with the progression of breast cancer to more invasive phenotypes. Additional studies are needed to address these evolving issues.

Inhibition of CAK stimulation of ER transactivation by MTA1 was presumably due in part to the recruitment of HDAC to the MTA1-CAK complex, because inhibition could be partially relieved by the HDAC inhibitor TSA. Also the CAK complex in breast cancer cells with deregulated MTA1 contained HDAC2 (Fig. 7). For the first time, these results show that CAK complex interacts with an HDAC-interacting corepressor MTA1. Because both CAK and MTA1 are known to target ER (7, 27), the findings presented here have revealed the existence of novel regulatory interactions between MTA1 and CAK and presented a novel control mechanism for ER transactivation functions in breast cancer cells. Chen *et al.* (27) have earlier shown that ER phosphorylation was induced by CDK7 and MAT1 in presence of estrogen. Our results are in agreement with that finding. Moreover, in the present study we have also demonstrated that phosphorylation of ER could be inhibited as a result of MTA1 overexpression both in presence and absence of the ligand. This illustrates the potential existence of an additional mechanism of MTA1-induced inhibition of CAK activity.

That the expression of MTA1 and MAT1 could be detected in ER-negative breast cancer cells and tissues other than the mammary gland (7) (Fig. 2) is important because it suggests that MTA1 might also influence the functions of MAT1 and/or the CAK complex in cellular functions other than ER transactivation. Because MAT1 modulation of CAK activity regulates cell cycle progression through G_1 (24), the effect of MTA1 on these events in ER-negative breast cancer cells remains to be investigated in the future studies.

The finding that the ER coactivator MAT1 as a part of the CAK complex interacts with MTA1, an ER corepressor, is surprising, because it raises the possibility that the final outcome of the ER transactivation function is influenced by complex protein-protein interactions rather than by isolated interaction with one class of proteins. It has been proposed that different HDAC complexes might be recruited for simple deacetylation of dynamically regulated ER target gene promoters. The associated nonenzymatic activities may play a role in determining the nature of the repression. From our results, it appears that MTA1 has inhibitory activity against MAT1/CAK-mediated interaction/stimulation of ER transactivation. Because MTA1 exhibited an overall corepressor function in the presence of CAK and E2 stimulation, these findings suggested an additional mechanism of MTA1 suppression of ER transactivation in breast cancer cells.

In summary, the present study identified MAT1 as a target of corepressor MTA1 and provided new evidence to suggest that the transactivation functions of ER are influenced by the regulatory interactions between CAK and MTA1. Our findings are in agreement with emerging models suggesting the existence of corepressor and coactivators are in the same complex. This model suggests that MTA1 and MAT1 might transmodulate the functions of ER and that any potential deregulation of MTA1 is likely to contribute to the functional inactivation of the ER pathway, presumably by recruitment of MTA1 to the ER target promoter chromatin.

REFERENCES

1. Berger, S. L. (2002) *Curr. Opin. Genet. Dev.* **12,** 142–148
2. Owen-Hughes, T., and Workman, J. L. (1994) *Crit. Rev. Eukaryotic Gene Expression* **4,** 403–441
3. Owen-Hughes, T., Utley, R. T., Cote, J., Peterson, C. L., and Workman, J. L. (1996) *Science* **273,** 513–516
4. Paranjape, S. M., Kamakaka, R. T., and Kadonaga, J. T. (1994) *Annu. Rev. Biochem.* **63,** 265–297
5. Brownell, J. E., Zhou, J., Ranalli, T., Kobayashi, R., Edmondson, D. G., Roth, S. Y., and Allis, C. D. (1996) *Cell* **84,** 843–851
6. Lomvardas, S., and Thanos, D. (2002) *Mol. Cell* **9,** 209–211
7. Mazumdar, A., Wang, R. A., Mishra, S. K., Adam, L., Bagheri-Yarmand, R., Mandal, M., Vadlamudi, R. K., and Kumar, R. (2001) *Nat. Cell Biol.* **3,** 30–37
8. Hassig, C. A., Fleischer, T. C., Billin, A. N., Schreiber, S. L., and Ayer, D. E. (1997) *Cell* **89,** 341–347
9. Laherty, C. D. Yang, W.-M., Sun, J.-M., Davie, J. R., Seto, E., and Eisenman, R. N. (1997) *Cell* **89,** 349–356
10. Xue, Y., Wong, J., Moreno, G. T., Young, M. K., Cote, J., and Wang, W. (1998) *Mol. Cell* **2,** 851–861
11. Zhang, Y., Ng, H. H., Erdjument-Bromage, H., Tempst, P., Bird, A., and Reinberg, D. (1999) *Genes Dev.* **13,** 1924–1935
12. Toh. Y., Pencil, S. D., and Nicolson, G. L. (1994) *J. Biol. Chem.* **269,** 22958–22963
13. Tassan, J. P., Jaquenoud M., Fry, A. M., Frutiger, S., Hughes, G. J., and Nigg, E. A. (1995) *EMBO J.* **14,** 5608–5617
14. Morgan, D. O. (1997) *Annu. Rev. Cell Dev. Biol.* **13,** 261–291
15. Nigg, E. A. (1996) *Curr. Opin. Cell Biol.* **8,** 312–317
16. Reardon, J. T., Ge, H., Gibbs, E., Sancar, A., Hurwitz, J., and Pan, Z. Q. (1996) *Proc. Natl. Acad. Sci. U. S. A.* **93,** 6482–6487
17. Busso, D., Keriel, A., Sandrock, B., Poterszman, A., Gileadi, O., and Egly, J. M. (2000) *J. Biol. Chem.* **275,** 22815–22823
18. Reardon, J. T., Ge, H., Gibbs, E., Sancar A., Hurwitz, J., and Pan, Z. Q. (1996) *Proc. Natl. Acad. Sci. U. S. A.* **93,** 6482–6487
19. Devault, A., Martinez, A. M., Fesquest D., Labbe, J. C., Morin, N., Tassan, J. P., Nigg, E. A., Cavadore, J. C., and Doree, M. (1995) *EMBO J.* **14,** 5027–5036
20. Larochelle, S., Chen, J., Knights, R., Pandur, J., Morcillo, P., Erdjument-Bromage, H., Tempst, P., Suter, B., and Fisher, R. P. (2001) *EMBO J.* **20,** 3749–3759
21. Rossignol, M., Kolb-Cheynel, I., and Egly, J. M. (1997) *EMBO J.* **16,** 1628–1637
22. Inamoto, S., Segil, N., Pan, Z. Q., Kimura, M., and Roeder, R. G. (1997) *J. Biol. Chem.* **272,** 29852–29858

23. Ko, L. J., Shieh, S. Y., Chen, X., Jayaraman, L., Tamai, K., Taya, Y., Prives, C., and Pan, Z. Q. (1997) *Mol. Cell. Biol.* **17,** 7220–7229
24. Wu, L., Chen, P., Shum, C. H., Chen, C., Barsky, L. W., Weinberg, K. I., Jong, A., and Triche, T. J. (2001) *Mol. Cell. Biol.* **21,** 260–270
25. Rochette-Egly, C., Adam, S., Rossignol, M., Egly, J. M., and Chambon, P. (1997) *Cell* **90,** 97–107
26. Bastien, J., Adam-Stitah, S., Riedl, T., Egly, J. M., Chambon, P., and Rochette-Egly, C. (2000) *J. Biol. Chem.* **275,** 21896–21904
27. Chen, D., Riedl, T., Washbrook, E., Pace, P. E., Coombes, R. C., Egly, J.-M., and Ali, S. (2000) *Mol. Cell* **6,** 127–137
28. Kumar, R., Wang, R.-A., Mazumdar, A., Talukder, A. H., Mandal, M., Yang, Z., Bagheri-Yarmand, R., Sahin, A., Hortobagyi, G., Adam, L., Barnes, C. J., and Vadlamudi, R. K. (2002) *Nature* **418,** 654–657
29. Li, F., Adam, L., Vadlamudi, R. K., Zhou, H., Sen, S., Chernoff, J., Mandal, M., and Kumar, R. (2002) *EMBO Reports* **3,** 767–773
30. Wang, R-A., Mazumdar, A., Vadlamudi, R. K., and Kumar, R. (2002) *EMBO J.* **21,** 5437–5447.
31. Vadlamudi, R. K., Wang R. W., Mazumdar, A., Kim, Y. S., Shin, J, Sahin, A., and Kumar, R. (2001) *J. Biol. Chem.* **276,** 38272–38279
32. Barnes, C. J., Li, F., Mandal, M., Yang, Z., Sahin, A. A., and Kumar, R. (2002) *Cancer Res.* **62,** 1251–1255
33. Korsisaari, N., and Makela, T. P. (2000) *J. Biol. Chem.* **275,** 34837–34840

MTA1 Interacts with MAT1, a Cyclin-dependent Kinase-activating Kinase Complex Ring Finger Factor, and Regulates Estrogen Receptor Transactivation Functions

Amjad H. Talukder, Sandip K. Mishra, Mahitosh Mandal, Seetharaman Balasenthil, Sonal Mehta, Aysegul A. Sahin, Christopher J. Barnes and Rakesh Kumar

J. Biol. Chem. 2003, 278:11676-11685.
doi: 10.1074/jbc.M209570200 originally published online January 13, 2003
